Karlsruhe Institute of Technology

Numerical Calculation of Specific Energy Distribution of I-125 in Water with Geant4, Using Different Frequency Distributions

by Bernd Heide[1]

KIT SCIENTIFIC WORKING PAPERS 71

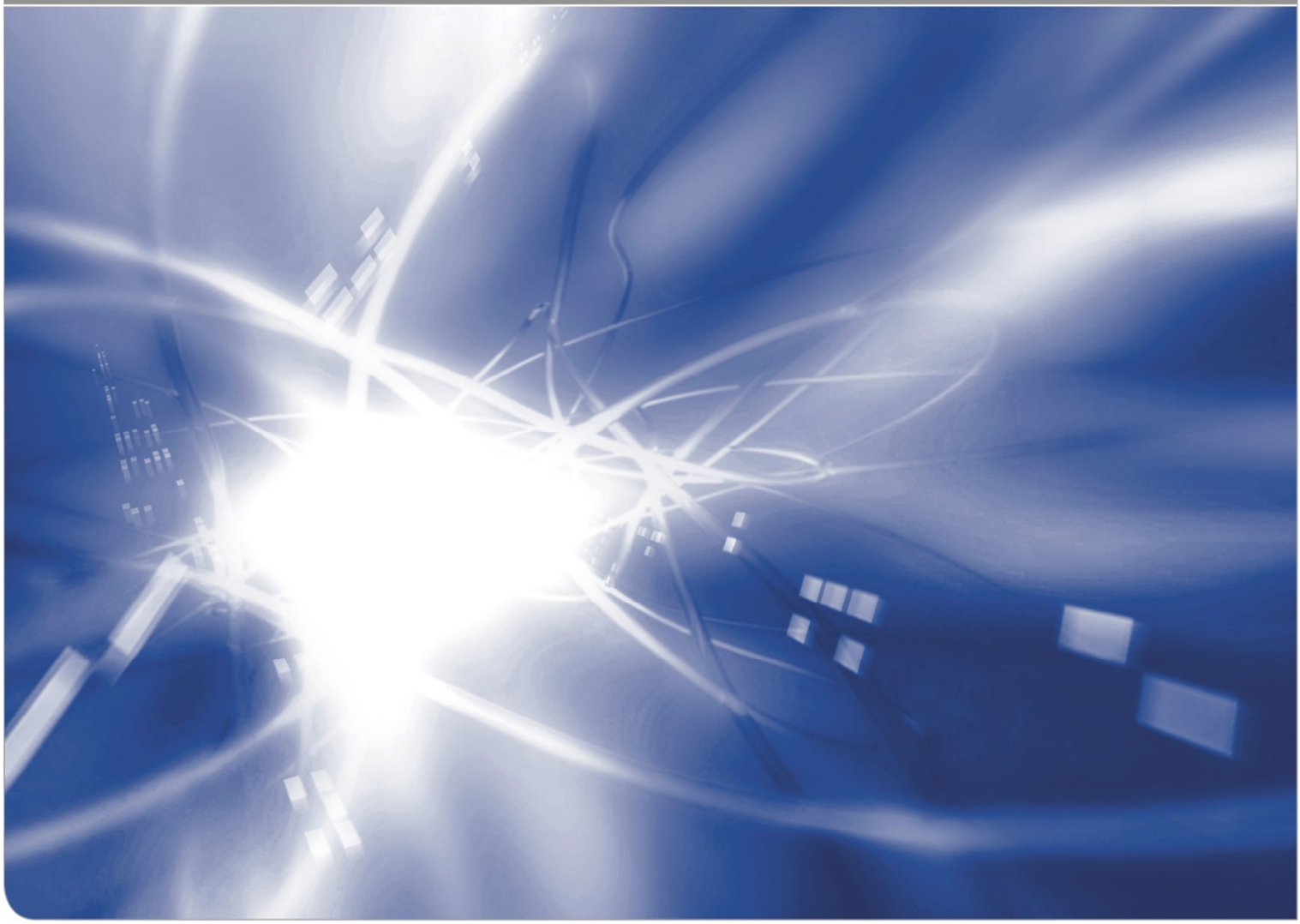

[1] Institut für Nukleare Entsorgung

Impressum

Karlsruher Institut für Technologie (KIT)
www.kit.edu

2017

ISSN: 2194-1629

Numerical Calculation of Specific Energy Distribution of I-125 in Water with Geant4, Using Different Frequency Distributions

(B. Heide, Karlsruhe Institute for Technology, Institute for Nuclear Waste Disposal)

Abstract

The specific energy distributions in water caused by I-125 atoms, located in the centre of a sphere with a radius of 5 µm, were calculated using geant4. The dependence of the specific energy on the respective electron frequency distributions was investigated, since there has been a lack of knowledge of the explicit electron frequency distribution up to now. The electron frequency distribution was modelled as Poisson, log-normal, or uniform distribution. Among others, some differences in the specific energy distribution were found. The lowest average specific energy, however, was within the range of the highest average specific energy and vice versa.

I. Introduction

The specific energy is a fundamental quantity in microdosimetry — a dosimetry tailored to low-dose ionizing radiation. Low-dose ionizing radiation may be defined as a radiation causing a dose of 100 mSv or less (cf. Ref. [1]). Low-dose ionizing radiation has attracted intensive scientific research as not only workers in the nuclear industry but also the general population (in respect of diagnostic radiation examinations, for example) are affected by it.
The specific energy was introduced as a consequence of the fact that the absorbed dose is no longer fully adequate in general for leptons, photons, and hadrons impinging on human tissue if their interactions are related to volumes in the order of micrometers or smaller (cf. Ref. [2])[1].
The specific energy z is contained in the definition of the absorbed dose $\boldsymbol{D}$. $\boldsymbol{D}$ is a non-stochastic quantity defined as the limit of the quotient of the expectation value $\langle\Delta E\rangle$ of absorbed energy ΔE and the mass element Δm, where ΔE^2 was absorbed within Δm:

$$D = \lim_{\Delta m \to 0} \left(\frac{\langle \Delta E \rangle}{\Delta m} \right) \tag{1}$$

The limit is due to the fact that a radiation field is defined for every point in space and hence the dose should be defined for every point in space as well. The expectation value $\langle\Delta E\rangle$, it depends on Δm, avoids fluctuations of the quantity $\Delta E / \Delta m$, which arise when the mass element enters micrometer dimensions (and which become bigger and bigger when it gets smaller and smaller). The limit $\boldsymbol{D}$ exists in this way. Though the average value $\boldsymbol{D}$ does not any more necessarily represent the risk associated with low dose, since the expectation value can be quite different from the actual dose value of the small volume considered.
The specific energy z is just defined as the above mentioned stochastic quantity $\Delta E / \Delta m$,

[1] An estimation of radiation damage of human tissue caused by heavier ions, which even takes radicals and shock waves into account, can be found in Ref. [3].
[2] In a detailed view (cf. Ref. [4]), ΔE is termed 'energy imparted'. We shall not do so in favour of a simple representation.

$$z := \frac{\Delta E}{\Delta \mathrm{m}} \quad . \tag{2}$$

In order to better characterize the risk at low doses, the absorbed dose ***D*** should be replaced by the distribution *f(z)* of the specific energy for mass elements of micrometer dimensions or smaller.

In the following, we shall calculate the specific energy distribution for a sphere of water with a radius of 5 µm caused by I-125 atoms. The nuclide I-125 is of special interest in nuclear medicine and radiobiology owing to its extreme radiotoxicity caused by its low energy Auger electrons which provoke a highly localized energy deposition. The choice of I-125, and the present work as well, was last but not least motivated by Ref. [5].
Unfortunately there are no experimental electron spectra available for I-125 (cf. Ref. [6]). And in addition, there is an open question whether neutralization during the cascades should be considered or not (s. Ref. [6]). Therefore, we shall investigate how sensitive the specific energy distribution is to the electron frequency distribution. The electron frequency shall be modelled by means of a uniform, a log-normal, and a Poisson distribution. Furthermore, we shall demonstrate the effect when the two most probable electron energies are taken into account only.

II. Scenario

We shall apply the following scenario (cf. Ref. [5]). A point source of I-125 is placed at the centre of a sphere of water with radius r = 5 µm. Only electron emission is considered; photon emission is neglected. The electron spectrum is taken from Ref. [7]. A visualization of the scenario can be seen on Fig. 1 in Section VIII.

III. Computational Details

Our Monte Carlo simulations were performed using Geant4 (version 10.01, patch-01; s. Ref.[8]) running on the virtual machine 'VMware Player' (version 6.0.4 build-2249910; cf. Ref. [9]) hosted on an 'Intel®Core™ i7-3770 CPU@3.40 GHz' computer containing 32 GB RAM and the operating system Windows 7, 64-bit 6.1.7601. Furthermore, the Low Energy Electromagnetic Physics Package (containing the Livermore Data Libraries) was applied (cf. Ref. [10]). The range cut was 1 nm, the energy threshold was 990 eV. In addition, several small own computer programs were written for the peripheral work (e. g., in order to sample the directions of the source particles [here 'bunch effects' coming from uniform selection of spherical coordinates were avoided]).

IV. Calculation

We shall consider two approaches, '**A1**' and '**A2**', for calculating the specific energy distribution. The recipe of approach **A1** reads:

-- Consider all possible 15 electron channels (s. Ref. [7]) for one decay.

-- Calculate partial specific energy distribution $f_i(z)$ for each event *i*, where event *i* consists of a decay resulting in *i* emitted electrons. The index *i* ranges from 1 to 45.

-- Calculate *f(z)* according to $f(z) = \sum_{i=1}^{45} p_i * f_i(z)$,
where the values p_i are the function values of either a uniform function, a log-normal function, or a Poisson function, cf. above.

The recipe of approach **A2** is equal to **A1** except for the amount of electron channels per decay. Now either 12.241 keV electrons (Auger and Coster-Kronig, CK) with a yield of 24.90% or 7.242 keV electrons (internal conversion, IC) with a probability of 0.94% (cf. Ref. [5]) are taken into account only.

Please note that for a simulation task consisting of generation of only one specific-energy spectrum based on a distinct frequency distribution some CPU time may be saved when *i* is directly chosen due to the respective probability distribution instead of weighting $f_i(z)$ with p_i. We want, however, calculate specific-energy spectra for several different frequency distributions. Therefore, we make use of weighting $f_i(z)$ with p_i by which a lot of CPU time can be saved in general (since one simulation task only has to be done instead of several ones). Another advantage of weighting $f_i(z)$ with p_i is due to the fact that one also can easily investigate the effect of different frequency distributions on the specific-energy spectrum since the values of the one frequency distribution act on exactly the same $f_i(z)$ as do the values of the other one.

Besides the uniform frequency distribution, the log-normal distribution and the Poisson distribution are used. This is due to Ref. [6]. We found that the frequency distribution of the number of emitted electrons of Ref. [6] is well fitted by a log-normal distribution for the 'condensed phase', and follows excellently a Poisson distribution for the 'gaseous phase', cf. Figs. 2 and 3 in Section VII.
In addition to the values of the frequency distributions of the statistical universes, we also make explicitly use of the values of the respective simulated statistical sample contained in Ref. [6].

V. Simulated Results

The results are based either on the frequency distributions shown in Fig. 4 (Section VII) or on the uniform frequency distribution. The average value av = 2.98 was calculated by means of the simulated data (compare Ref. [6]). The average value av = 3.02 corresponds to av = 21.05 while the average value of 3.23 corresponds to av = 25.84 {= 24.9 (total yield of Auger and Coster-Kronig electrons per decay, cf. Ref. [5]) + 0.94 (total yield of internal conversion electrons per decay, s. Ref. [5])} in a way that the parameters of the density of the log-normal distribution (i. e. standard deviation σ and the average value μ) were calculated by

$$\sigma = \sqrt{\ln(\frac{\sigma_{ln}^2}{\mu_{ln}^2} + 1\,)} \qquad \text{and} \tag{3}$$

$$\mu = \ln(\mu_{ln}) - \sigma^2/2 \tag{4}$$

(s. Ref. [11])[3] where σ_{ln} and μ_{ln} (the standard deviation and the average value of the corresponding log-normal distributed quantity) were approximated by the respective Poisson distribution using $\sigma_{ln} = \sigma_{Poisson} = (\mu_{ln} = \mu_{Poisson})^{1/2}$.

In order to compare our calculated curves to each other, we make use of an Euclidean metric *d* on a (respective) metric space *M*, which we define as

$$d = \sqrt{\sum(\phi_i - \varphi_i)^2}\,, \tag{5}$$

with ϕ_i , $\varphi_i \in M \;\; \forall i \in N$ (N denotes the set of natural numbers). Furthermore, we calculate average values z_{av} of the specific energy. The uncertainty of z_{av} is one standard deviation.
If otherwise stated, the approach **A1** was used and the electron sampling was done indirectly.

According to Fig. 4, the log-normal distribution with average value av = 2.98, Log-norm_0, matches quite well with the simulated frequency distribution of Pomplun, termed Pomplun. The Pomplun distribution leads to an average electron number of 21.05. The metric d between the two curves reads d = 0.0399. The difference in the frequency distribution is nearly not visible with respect to the corresponding z·f(z) distributions, shown in Fig. 5. The metric between the two z·f(z) curves is d = 0.1842 (please note the diverse spaces). Both the Pomplun distribution and the distribution Log-norm_0 lead to the same specific energy:
z_{av} = (4.51 ± 1.97) mGy.

If the Pomplun curve in Fig. 4 is approximated by a Poisson distribution with the same average value, termed Poisson_1, the value of the metric is d = 0.0735. The z·f(z) distribution referring to Poisson_1 differs a little bit more from that of Pomplun than the aboved mentioned distribution Log-norm_0. This is seen in Fig. 6. The metric for this case reads d = 0.4634. Similar results were found with respect to the frequency distribution Log-norm_1 (s. Fig. 4 and Fig. 7). The average value of the specific energy is z_{av} = (4.32 ± 1.98) mGy for both curves (Poisson_1 and Log-norm_1).

The most obvious deviation from the Pomplun distribution of Fig. 4, besides of the uniform distribution, is accomplished by the Poisson distribution Poisson_2 as well as the log-normal distribution Log-norm_2. The average electron number of Poisson_2 reads 25.84. The metric between Pomplun and Poisson_2 is d = 0.1450. The difference between the z·f(z) curve which is based on Poisson_2 and the one which is related to Pomplun is quite visible. This can be inferred from Fig. 8. On that issue, the metric is d = 1.0207. Again similar results were found with respect to the frequency distribution Log-norm_2 (s. Fig. 4 and Fig. 9).
The average value of the specific energy amounts to z_{av} = (5.04 ± 1.95) mGy with respect to the distribution Poisson_2. The distribution Log-norm_2 leads to z_{av} = (5.03 ± 1.95) mGy.

Without any doubt, the largest deviation from the simulated data of Pumplun (s. Ref. [6]) is given by the uniform distribution. The metric equals to d = 6.5606 in this case. In terms of Fig. 10, the metric is d = 1.5987. The graphs of Fig. 10 demonstrate also a big difference

[3] Instead of '$\exp[2\mu+2\sigma^2] - \exp[2\mu+2\sigma^2]$', the term '$\exp[2\mu+2\sigma^2] - \exp[2\mu+\sigma^2]$' was used.

between the centres of gravity of the curves. The average value of the specific energy based on the uniform frequency distribution is the highest one: $z_{av} = (5.45 \pm 1.94)$ mGy.

Please note that the lowest value of the average specific energy, $z_{av} = 4.32$ mGy, is within the range of the highest one: $z_{av} = 4.32$ mGy $>$ $(5.45 - 1.94)$ mGy. And vice versa, the highest value, $z_{av} = 5.45$ mGy, is within the range of the lowest one, i. e. $z_{av} = 5.45$ mGy $<$ $(4.32 + 1.98)$ mGy.
The thing which is also worth to remark is, as the risk at low doses is characterized by means of the specific energy (cf. section Introduction), that the heights of the peaks of the $z \cdot f(z)$ curves change obviously with electron frequency distribution. This is demonstrated in Figs 11 and 12.
Last but not least we would like to point out that the first two peaks in the $z \cdot f(z)$ curves seem to vanish if 12.241 keV electrons (24.90% yield) and 7.242 keV electrons (0.94% yield) are taken into account only (approach **A2**). This may be inferred from Fig. 13. However, the $z \cdot f(z)$ curve labeled as 'PS' (**PS** ≡ **P**oisson distribution with average value 25.84, **S**caled) was generated by applying a shift of 8 mGy and a scaling value of 0.012 (using a direct sampling of the electrons). This was done in order to reduce artificial influence coming from scaling the sum of the electron yields to one[4]. In this respect, the shape of the PS curve should only serve as a possible indication.

VI. Summary and Conclusion

We calculated the specific energy distribution in water caused by I-125 atoms located in the centre of a sphere. Since there are no experimental electron spectra available, we investigated how sensitive the specific energy distribution is to the electron frequency distribution. The electron frequency was modelled by means of a uniform, a log-normal, and a Poisson distribution. Instead of sampling the electron frequency distributions directly, we calculated partial specific energy distributions and weighted them with the values of the respective electron frequency function in all but one cases. A direct sampling of the electron frequency was done once. The indirect sampling was of advantage concerning both the needed CPU time and the study of the effect of different frequency distributions (since the values of the one frequency distribution acted on exactly the same partial $f_i(z)$ as did the values of the other one).
We defined a metric as well as calculated average values of the specific energy for our investigation. We found some differences in the specific energy distributions which were due to the used electron frequency distribution. However, the lowest average specific energy was within the range of the highest average specific energy and vice versa. We conclude (by comparing the respective values of d) that the variation in the specific energy distribution is less than the variation in the electron frequency distribution.
Furthermore, we discussed the case when the two most probable electron energies are taken into account only. We found indication that the first two peaks in the $z \cdot f(z)$ curve vanish in this case.

[4] The scaling of the sum of the electron yields was also done for approach **A1**. It turned out, however, that the influence was negligible (due to the fact that the kinetic energy of the prominent electrons was relatively low).

VII. Figures

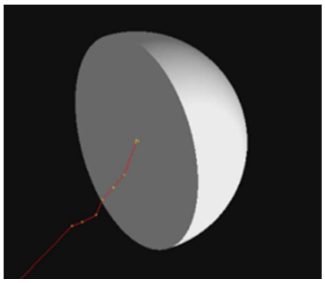

Figure 1. Visualisation of simulation scenario. Cutting of a sphere of water containing a I-125 source in its centre. The red line refers to an electron, the yellow dots illustrate interaction points.

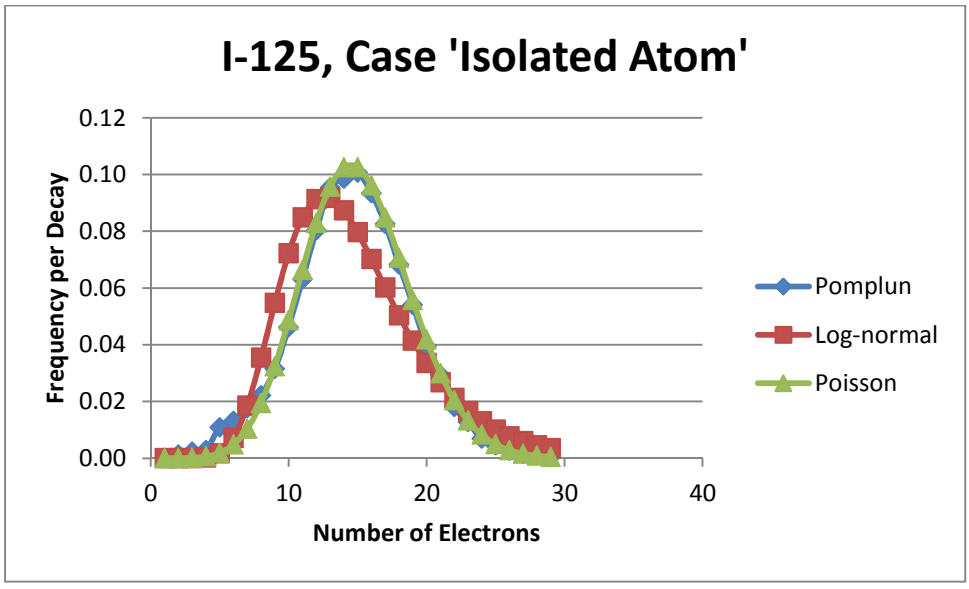

Fig. 2: Frequency distributions of the number of emitted electrons for case 'isolated atom'. Simulated data taken from Pomplun (cf. Ref. [6]). Data were fitted with both a log-normal distribution and a Poisson distribution. The Poisson distribution matches better with the data than the log-normal distribution.

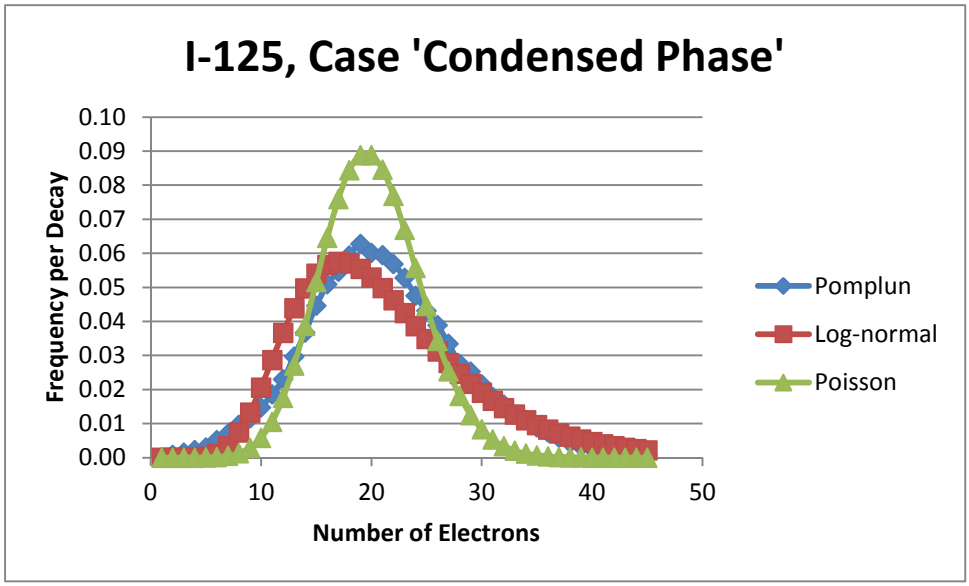

Fig. 3: Frequency distributions of the number of emitted electrons for case 'condensed phase'. Simulated data taken from Pomplun (cf. Ref. [6]). Data were fitted with both a log-normal distribution and a Poisson distribution. The log-normal distribution matches better with the data than the Poisson distribution.

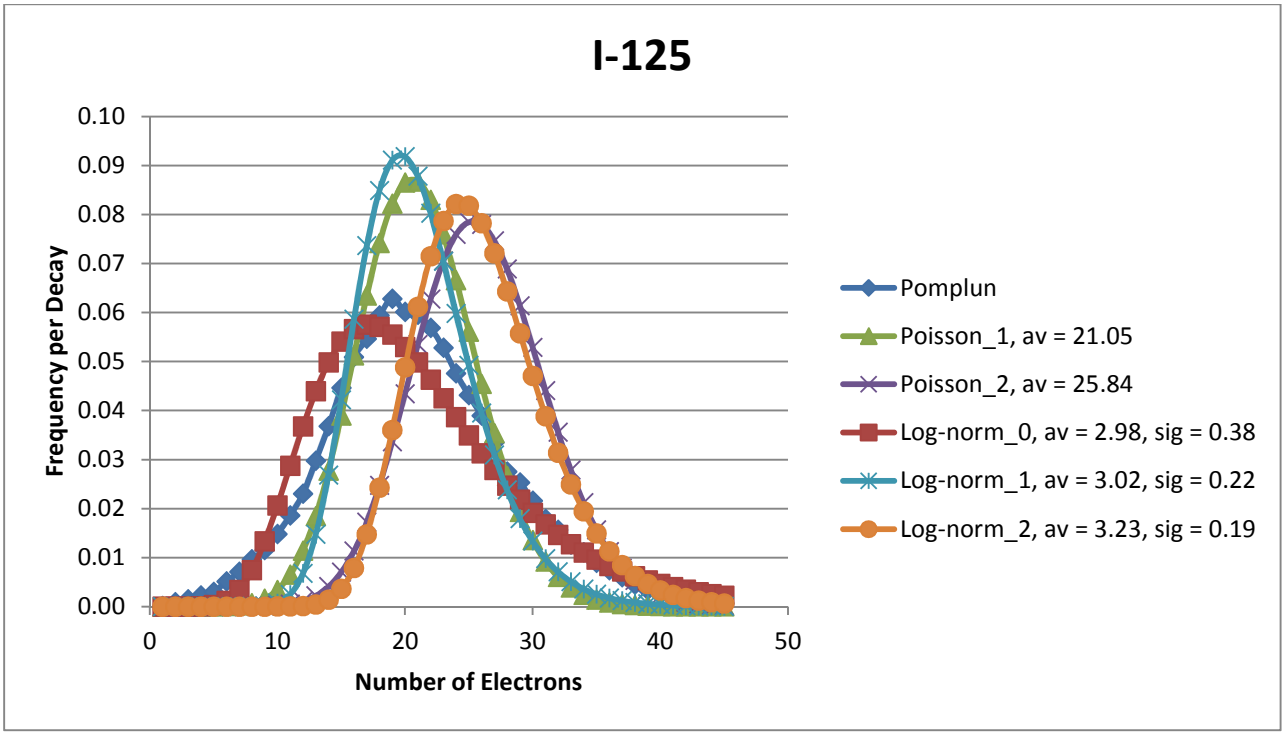

Fig. 4: Frequency distributions of the number of emitted electrons (case 'condensed phase') which were explicitly used. Simulated data taken from Pomplun (cf. Ref. [6]). Standard deviation is abbreviated by 'sig', the average value is denoted by 'av'. The expression 'Poisson' indicates a Poisson distribution, the term 'Log-norm' is used for a log-normal distribution.

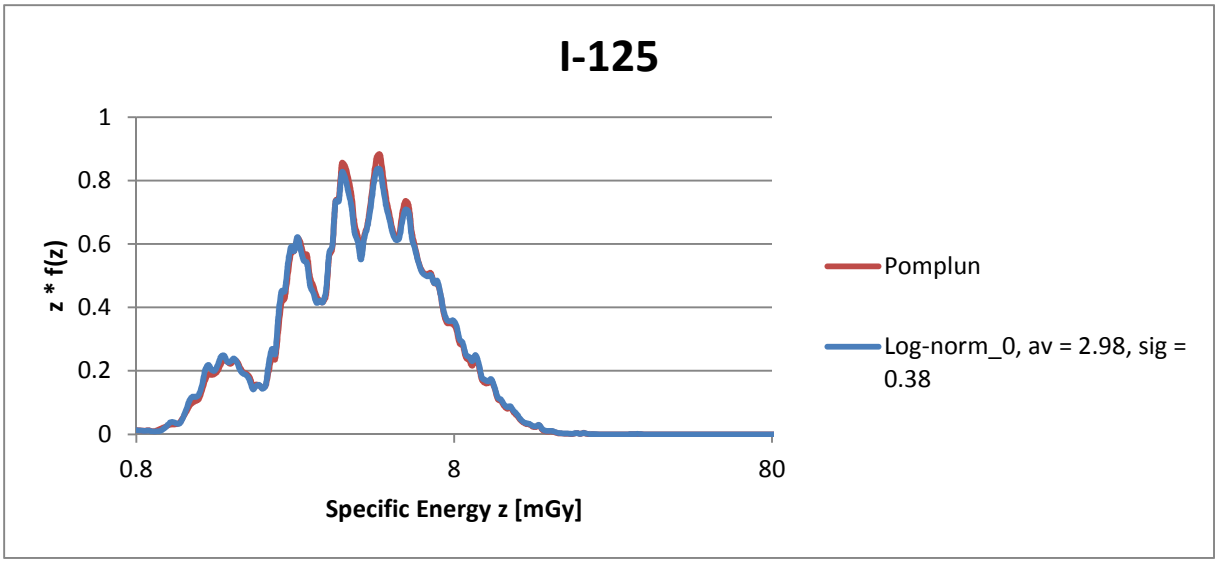

*Fig. 5: z·f(z) distributions for different frequency distributions using approach **A1**. Red curve refers to the frequency distribution of Pomplun (cf. Ref. [6]). Blue curve refers to a log-normal frequency distribution with an average value of 2.98 and a standard deviation of 0.38. Binning done according to Ref. [5].*

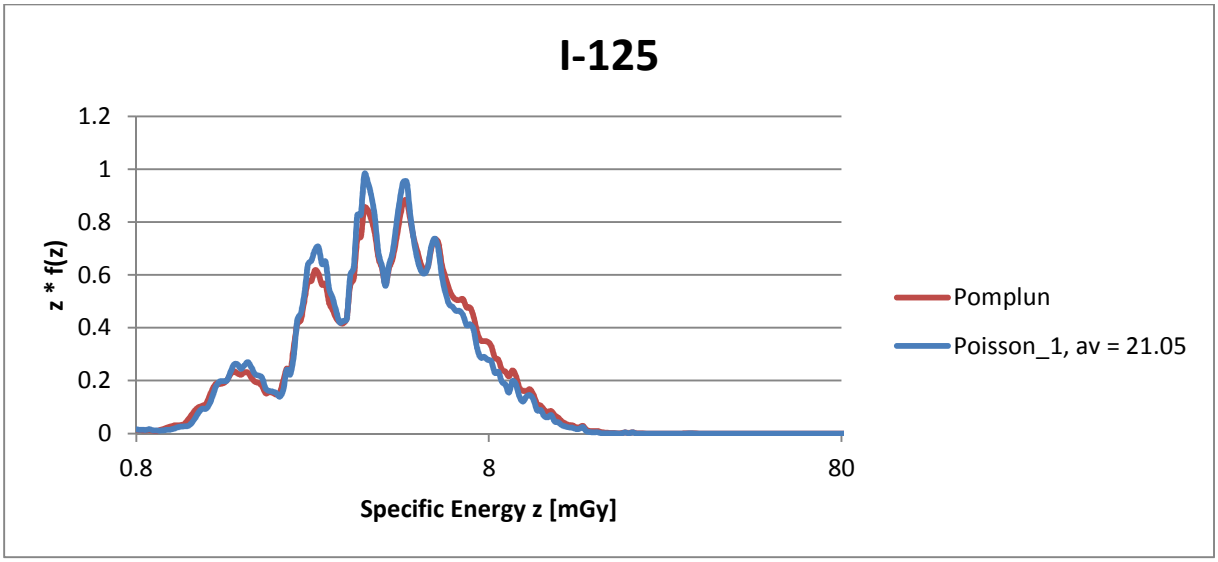

*Fig. 6: z·f(z) distributions for different frequency distributions using approach **A1**. Red curve refers to the frequency distribution of Pomplun (cf. Ref. [6]). Blue curve refers to a Poisson frequency distribution with an average value of 21.05. Binning done according to Ref. [5].*

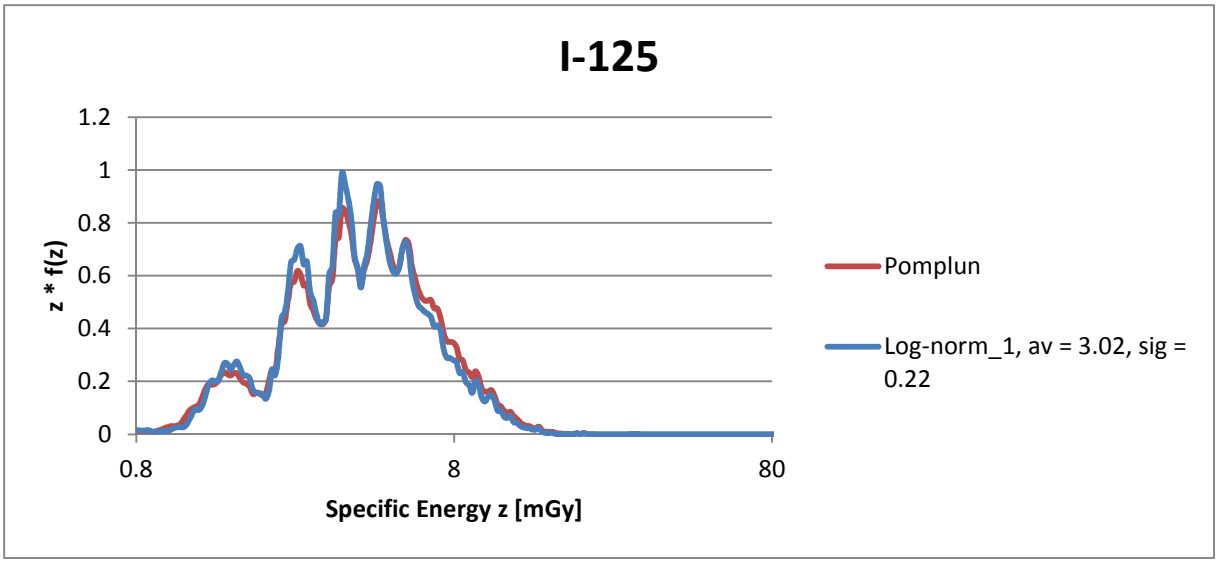

*Fig. 7: z·f(z) distributions for different frequency distributions using approach **A1**. Red curve refers to the frequency distribution of Pomplun (cf. Ref. [6]). Blue curve refers to a log-normal frequency distribution with an average value of 3.02 and a standard deviation of 0.22. Binning done according to Ref. [5].*

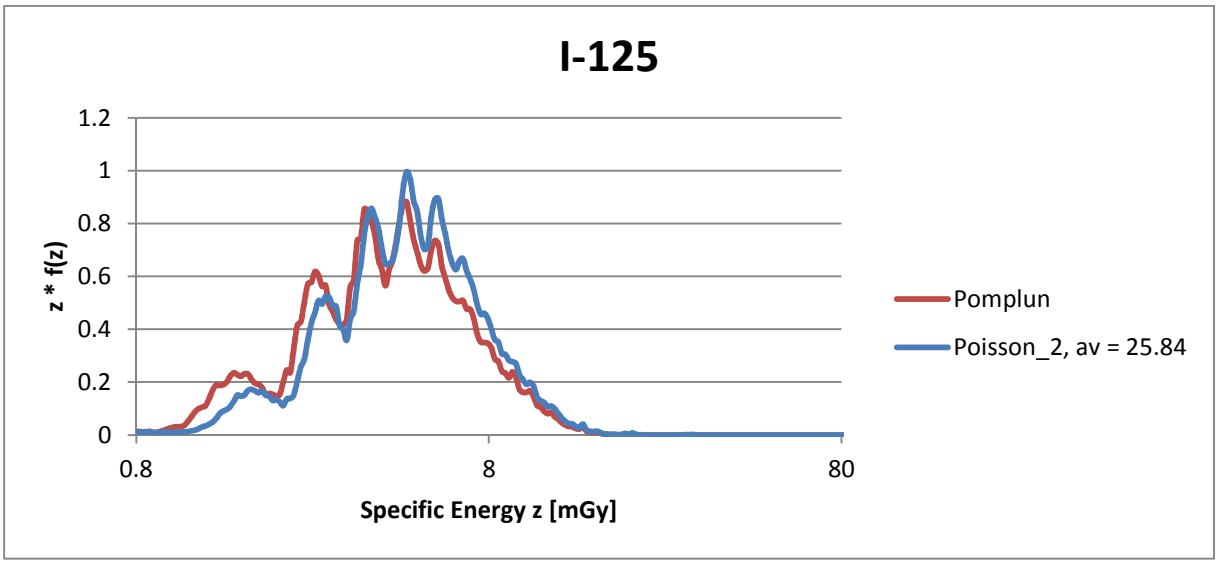

*Fig. 8: z·f(z) distributions for different frequency distributions using approach **A1**. Red curve refers to the frequency distribution of Pomplun (cf. Ref. [6]). Blue curve refers to a Poisson frequency distribution with an average value of 25.84. Binning done according to Ref. [5].*

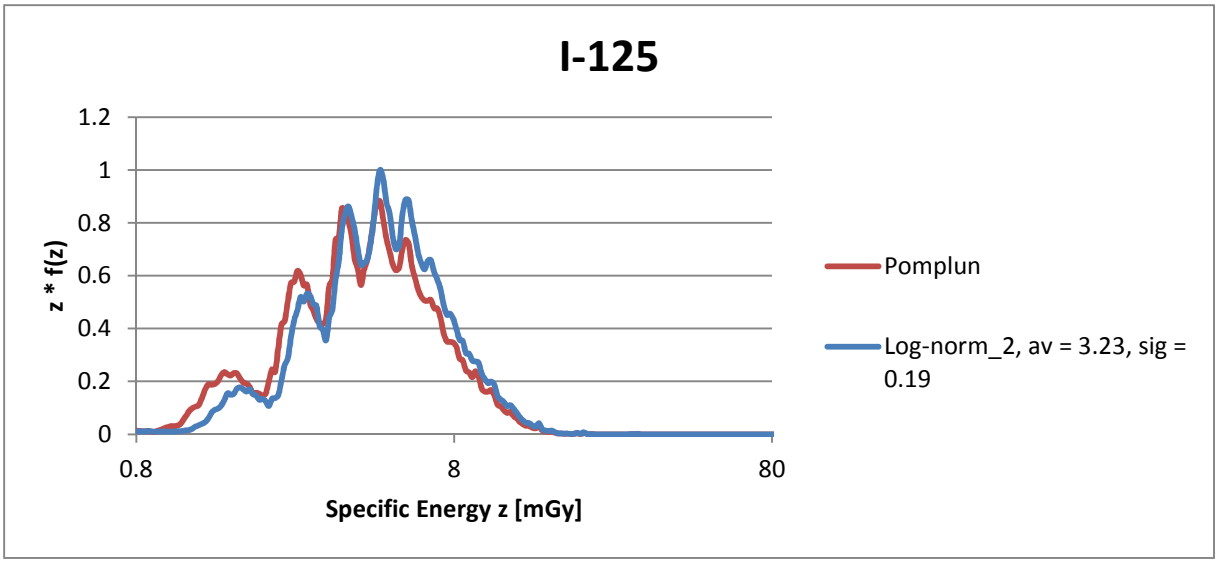

*Fig. 9: z·f(z) distributions for different frequency distributions using approach **A1**. Red curve refers to the frequency distribution of Pomplun (cf. Ref. [6]). Blue curve refers to a log-normal frequency distribution with an average value of 3.23 and a standard deviation of 0.19. Binning done according to Ref. [5].*

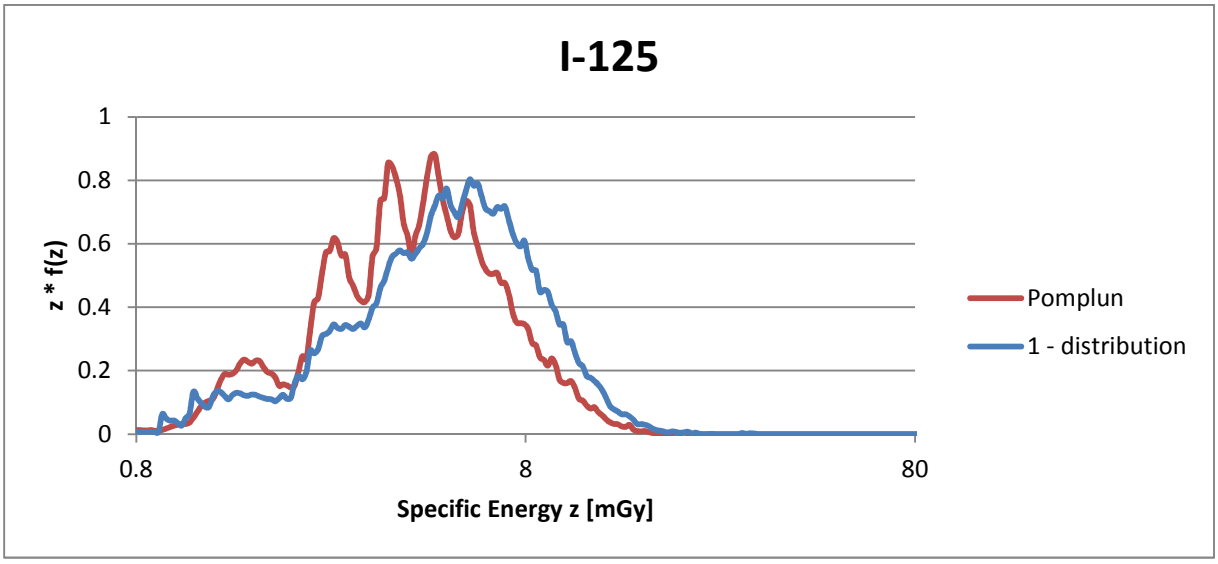

*Fig. 10: z·f(z) distributions for different frequency distributions using approach **A1**. Red curve refers to the frequency distribution of Pomplun (cf. Ref. [6]). Blue curve refers to the uniform distribution. Binning done according to Ref. [5].*

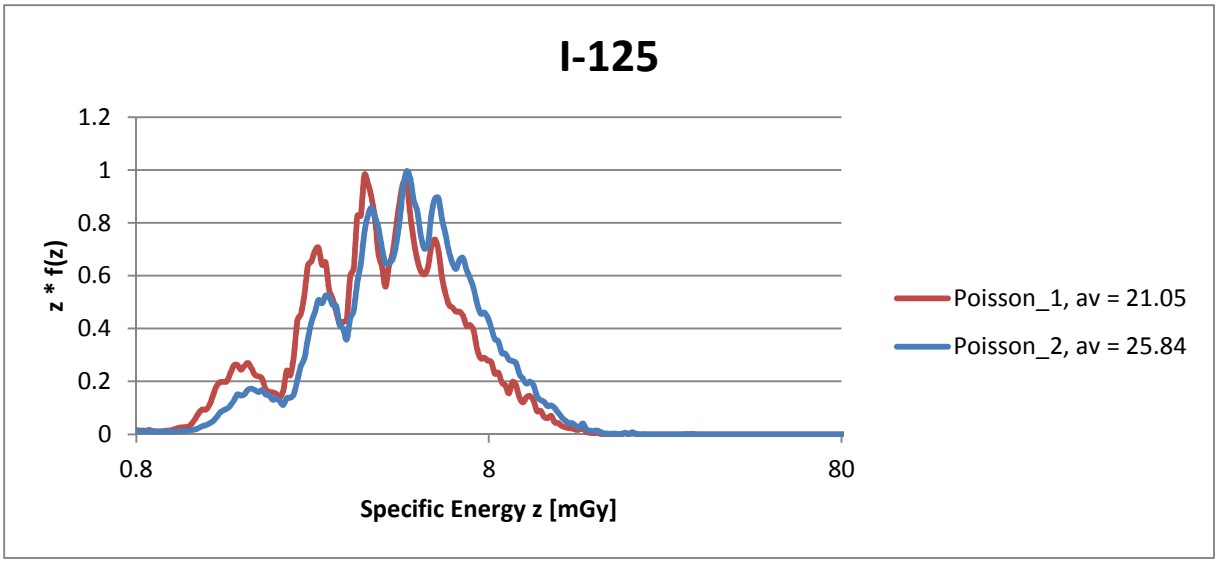

*Fig. 11: z·f(z) distributions for different frequency distributions using approach **A1**. Red curve refers to a Poisson frequency distribution with an average value of 21.05. Blue curve refers to a Poisson frequency distribution with an average value of 25.84. Binning done according to Ref. [5].*

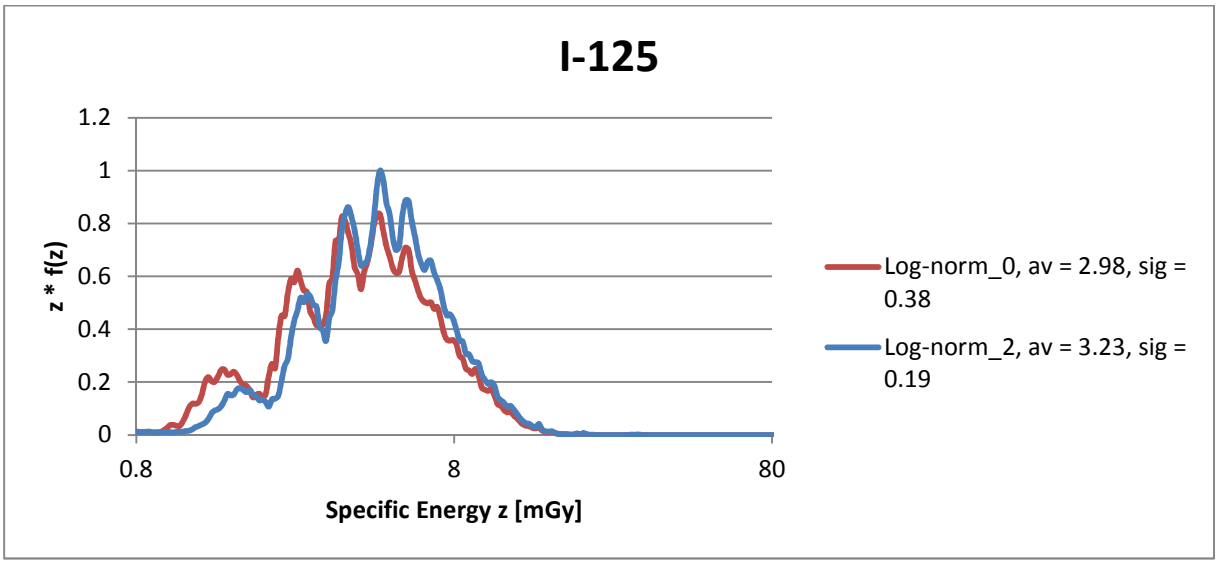

*Fig. 12: z·f(z) distributions for different frequency distributions using approach **A1**. Red curve refers to a log-normal frequency distribution with an average value of 2.98 and a standard deviation of 0.38. Blue curve refers to a log-normal frequency distribution with an average value of 3.23 and a standard deviation of 0.19. Binning done according to Ref. [5].*

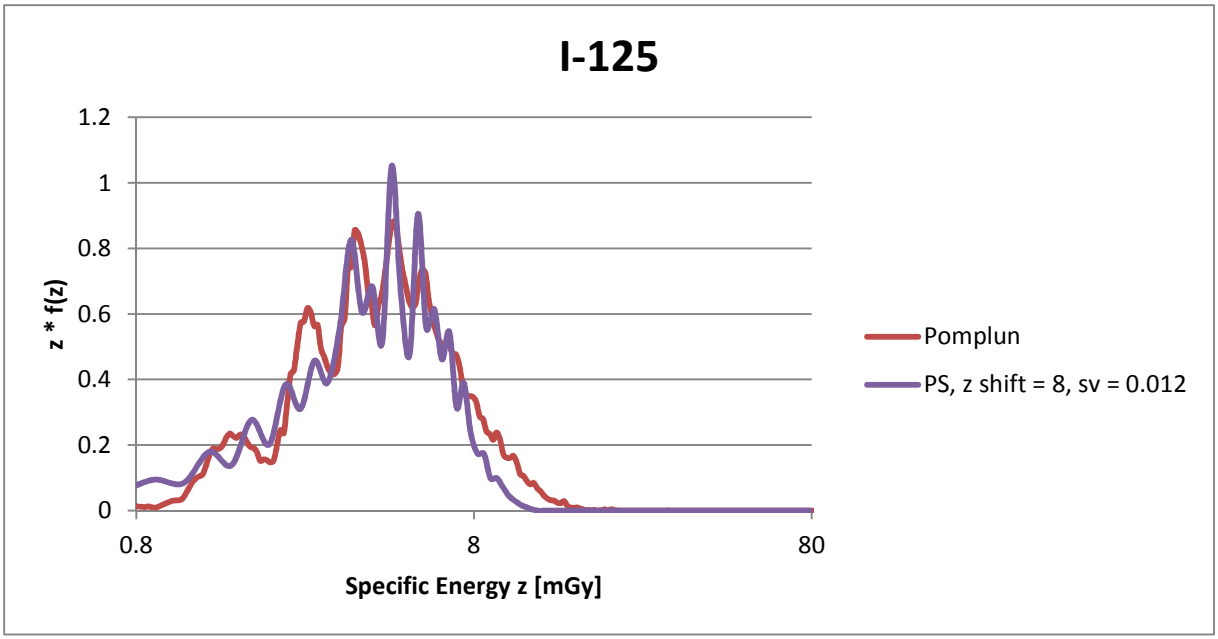

*Fig. 13: z·f(z) distributions for different frequency distributions. Red curve refers to the frequency distribution of Pomplun (cf. Ref. [6]); approach **A1** was used. Purple curve refers to a Poisson frequency distribution with an average value of 25.84; approach **A2** was used. The abbreviation PS means 'Poisson Sampled'. The electron sampling was performed directly. The purple curve was shifted by 8 mGy and scaled by a factor of 0.012. Binning done according to Ref. [5].*

References:

[1] Feng Ru Tang, Weng Keong Loke, and Boo Cheong Khoo: Low-Dose or Low-Dose-Rate Ionizing Radiation-Induced Bioeffects in Animal Models. Journal of Radiation Research, Vol. 58, No 2, 2017, pp. 165 – 182.

[2] H.H. Rossi and M. Zaider: Microdosymetry and Its Applications. Springer-Verlag Berlin (1996), ISBN 3 – 540 – 58541 – 9.

[3] E. Surdutovich and A. V. Solov'yov: Multiscale Approach to the Physics of Radiation Damage with Ions. Eur. Phys. J. D (2014) 68: 353, DOI: 10.1140/epjd/e2014-50004-0.

[4] F. H. Attix: Energy Imparted, Energy Transferred and Net Energy Transferred. Phys. Med. Biol., Vol. 28, No. 12, 1983, pp. 1385-1390.

[5] H. Rabus, C. Villagrasa, M. U. Bug, E. Gargioni, M. – C. Bordage, and B. Heide: Eurados Exercise on Uncertainty Assessment in Micro- and Nanodosimetry Using Monte – Carlo calculations. Information available on https://www.researchgate.net/project/Eurados-exercise-on-uncertainty-assessment-in-micro-and-nanodosimetry-using-Monte-Carlo-calculations (accessed 8 May 2017).

[6] E. Pomplun: Auger Electron Spectra - The Basic Data for Understanding the Auger Effect. Acta Oncologica, Vol. 39, No. 6, 2000, pp. 673-679.

[7] R. W. Howell: Radiation Spectra for Auger-Electron Emitting Radionuclides: Report No 2 of AAPM Nuclear Medicine Task Group No 6. Med. Phys. 19 (6) 1992, p. 1371.

[8] https://geant4.web.cern.ch/geant4/support/source_archive.shtml (accessed 12 July 2017).

[9] VMware, Inc., 3401 Hillview Ave, Palo Alto, CA 94304, USA, https://www.vmware.com (accessed 12 July 2017).

[10] http://citeseerx.ist.psu.edu/viewdoc/download?doi=10.1.1.470.828&rep=rep1&type=pdf (accessed 12 July 2017).

[11] A. M. Mood, F. A. Graybill, and D. C. Boes: Introduction to the Theory of Statistics. Third ed., Tokyo, McGraw-Hill Inc., 1974. pp. 540–541.

KIT Scientific Working Papers
ISSN 2194-1629

www.kit.edu